NANOVID TRACKING: A NEW AUTOMATIC METHOD FOR THE STUDY OF MOBILITY IN LIVING CELLS BASED ON COLLOIDAL GOLD AND VIDEO MICROSCOPY

HUGO GEERTS, MARK DE BRABANDER, RONNY NUYDENS, STAF GEUENS, MARK MOEREMANS, JAN DE MEY, AND PETER HOLLENBECK*

*Division of Cellular Biology and Chemotherapy, Department of Life Sciences, Janssen Pharmaceutica Research Laboratories, B-2340 Beerse, Belgium; *Medical Research Council Cell Biophysics Unit, London WC2B 5RL, United Kingdom*

ABSTRACT We describe a new automatic technique for the study of intracellular mobility. It is based on the visualization of colloidal gold particles by video-enhanced contrast light microscopy (nanometer video microscopy) combined with modern tracking algorithms and image processing hardware. The approach can be used for determining the complete statistics of saltatory motility of a large number of individual moving markers. Complete distributions of jump time, jump velocity, stop time, and orientation can be generated. We also show that this method allows one to study the characteristics of random motion in the cytoplasm of living cells or on cell membranes. The concept is illustrated by two studies. First we present the motility of colloidal gold in an in vitro system of microtubules and a protein extract containing a kinesin-like factor. The algorithm is thoroughly tested by manual tracking of the videotapes. The second study involves the motion of gold particles microinjected in the cytoplasm of PTK-2 cells. Here the results are compared to a study using the spreading of colloidal gold particles after microinjection.

INTRODUCTION

During the last few years, some elegant techniques for studying the lateral movement of molecules have been developed (Axelrod, 1976; Elson and Magde, 1974; Magde and Elson, 1974; Kapitza, 1985; Peters, 1984; Barak and Webb, 1982; Smith, 1979). They all use fluorescently labeled molecules, the time evolution of which can be followed by a variety of means. One of the main features of spectroscopic techniques is the use of concentrations of molecules, i.e., quantities that are related to the global number of molecules in a certain area, defined within the resolution of the chosen optics. This means that the global mobility behavior of a set of molecules is studied.

Ideally one would like to follow individual molecules to obtain exact information on this mobility. For this one needs a particular marker. Such a marker is colloidal gold, which has been very popular for morphological studies. One can indeed couple antibodies to specific molecules with colloidal gold probes and study the localization at the ultrastructural level (electron microscopy). Recently, a new approach, called NANOVID (nanoparticle video microscopy), has coupled the colloidal gold technology with light microscopy (De Brabander et al., 1985). It turns out that, despite the very small size of the gold probes (20–40 nm), single probes can be made visible in the light microscope by video-enhanced contrast techniques (Allen et al., 1981; Inoué, 1981). Essentially, the technique uses the potential of video microscopy to enhance contrast greatly by electronic subtraction of background intensity. Individual gold probes (20–40 nm) are observed with bright field illumination at maximal aperture. They are invisible to the eye but appear as clearly defined black dots on the video screen after contrast enhancement. They are unambiguously discerned from cellular organelles which produce no contrast at correct Köhler illumination because they are phase objects. The gold particles are visible because they scatter light out of the aperture of the optical system. We are now able to follow the motion of individual colloidal gold markers in living cells. Furthermore, by coupling this concept to the power of image processing technology and minicomputers, we can study statistics of different mobilities in great detail.

This work presents the automatic tracking approach and its application to two different experimental systems.

The first application is the study of the mobility of 40-nm gold probes in a microtubule system in vitro. The aim was to investigate the mechanism of saltatory motion, induced by a kinesin-like protein extract. This model system was chosen because we could easily check the results by manual tracking and because all motions (saltatory and random) turned out to be mainly one-dimensional, a very exciting result.

The second application is a demonstration of the measurement of cytoplasmic diffusion. Here we followed the spreading of colloidal gold particles shortly after microin-

jection in PTK-2 cells. This was analyzed by a classical two-dimensional diffusion equation. Some 2 h after microinjection, however, we could observe individual motion of single gold probes. By combining the two approaches, this system provided us with an internal check on the performance of the tracking approach, at least for the random motion.

MATERIALS

Cells

PTK-2 cells were cultured routinely in Eagle's minimal essential medium supplemented with non-essential amino acids and 10% fetal calf serum in a 5% CO_2 atmosphere. PTK-2 cells were seeded on 24 × 32 No. 0 coverslips.

Gold Probes

Colloidal gold particles of 40-nm diam were obtained from Janssen Life Sciences Products (Beerse, Belgium). They were stabilized with polyethyleneglycol (PEG) and bovine serum albumin (BSA) as described (De Mey, 1983). These particles have a negative surface charge (De Brabander et al., 1986).

Positively charged gold particles were prepared by incubating PEG-BSA gold with cethylpyridinium chloride (1 mg/ml) for 60 min. They showed a clear shift from anodic to cathodic migration in agarose gel electrophoresis.

Microinjection was done using a home-made version of the apparatus described by Ansorge (1982) on an inverted phase-contrast microscope using glass capillaries drawn to a tip opening of ±1 μm. Immediately after injection, the coverslips with the cells were removed from the petri dish and mounted on a slide using Parafilm strips as spacers and Valap (vaseline, lanoline, paraffin, ⅓ of each) to seal the microchamber.

All preparations were mounted on a Polyvar (Reichert Jung, Vienna) microscope, and the temperature of the preparation was kept at 37°C ± 1°C by an airstream incubator. The microscope was equipped with a universal condenser (numerical aperture [NA] 1.30) and a 100× planapo lens (NA 1.32).

Microtubules In Vitro

Tubulin free of microtubule-associated proteins was prepared from twice-cycled chick brain microtubule protein by the method of Murphy and Borisy (1975), dialyzed against 100 vol of PME (0.1 mM Pipes, 2.5 mM $MgSO_4$, 1 mM EGTA, pH 6.94) plus 0.1 mM GTP, and stored under liquid nitrogen.

The concentration of the stock solution was 7 mg/ml tubulin. For experiments the solution was diluted 20× with a 70 μM taxol buffer.

Spinal nerve roots free of their surrounding dura were obtained by dissection of fresh bovine spinal cords. They were homogenized in 1–2 vol of cold PME containing 1 mM dithiothreithol (DTT), 0.1 mM phenylmethylsulfonyl fluoride, and 0.5% protease inhibitor stock (0.2 mg/ml pepstatin A, 2 mg/ml soybean trypsin inhibitor, 2 mg/ml *p*-tosyl-L-arginine methyl ester, 2 mg/ml *N*-α-benzoyl-L-arginine methyl ester, 2 mg/ml L-1-tosylamide-phenylethylchloromethyl ketone, 0.2 mg/ml leupeptin). The homogenate was centrifuged at 30,000 *g* for 45 min, 4°C, and the supernatant was centrifuged again at 150,000 *g* for 90 min, 4°C. To this high speed supernatant was added 25% glycerol, 0.5 mM GTP, and 20 μM taxol. It was incubated at 30°C for 30 min to induce microtubule polymerization and then centrifuged at 100,000 *g* for 60 min, 30°C. The supernatant was discarded and the microtubule pellet washed by resuspension in 5 vol of PME plus taxol, glycerol, and DTT followed by centrifugation for 45 min at 100,000 *g*, 30°C. The washed microtubule pellet was then extracted by resuspension in 5–10 vol of PME plus glycerol, taxol, DTT, and 5 mM ATP, incubated 15 min, and then centrifuged as in the washing step. The ATP-released supernatant was dialyzed overnight at 4°C against 100 vol of PME containing 1 mM 2-mercaptoethanol and 0.1% protease inhibitor stock, and then applied to a gradient of 5–25% sucrose in the same buffer and centrifuged at 125,000 *g* for 6.5 h, 4°C. Fractions from the gradient were analyzed for protein content by SDS-polyacrylamide gel electrophoresis. Fractions containing the kinesin-like factor were dialyzed at 4°C against 100 vol of PME plus 1 mM 2-mercaptoethanol. The concentration of ATP, added to the solution before measuring, was 1 mM.

METHODS

Getting the Images

The set-up for video-enhanced microscopy has been described in detail elsewhere (De Brabander et al., 1985) (Fig. 1). Briefly, we use a Polyvar microscope supplemented with a Hamamatsu Photonics (C-1966; Hamamatsu City, Japan) video camera. This output is directed to a Hamamatsu C-1966 Image Processing System, where an analog offset is subtracted in real-time for contrast enhancement. The video image is digitized in a 512 × 512 pixel pattern of 8 bits deep. This digital information can then be processed by different means (mottle subtraction, jumping, or rolling average) before it is put on videotape by a Sony VO-5850 P video recorder. On the monitor, the colloidal gold particles are clearly seen as distinct entities with high contrast, especially when using normal bright-field optics (Fig. 2). Before each experiment, a calibration stage is used for calibrating the field of view. The Hamamatsu system is interfaced by a DR11-W DMA-module (Digital Equipment Corp., Marlboro, MA) to a VAX-11 725 system with 2 MByte RAM memory. The necessary software is based on the drivers included in the VMS operating system and is provided by Hamamatsu Photonics. For a given stretch of videotape, we transfer images in a straight sweep of 8 to 10 frames via the image processor to the computer system where we put them on disk. Due to different time delays, we can get an interframe time between 4 and 10 s. By interleaving several sweeps, we reduce this time resolution to the order of 500 ms. After each sweep, frames are read again from disk and are bit sliced by using a mask on the histogram of the gray-level. The mask (n_0, n_1) on the histogram is slightly adjusted to anticipate illumination fluctuations by trying to keep the second moment constant over total acquisition time.

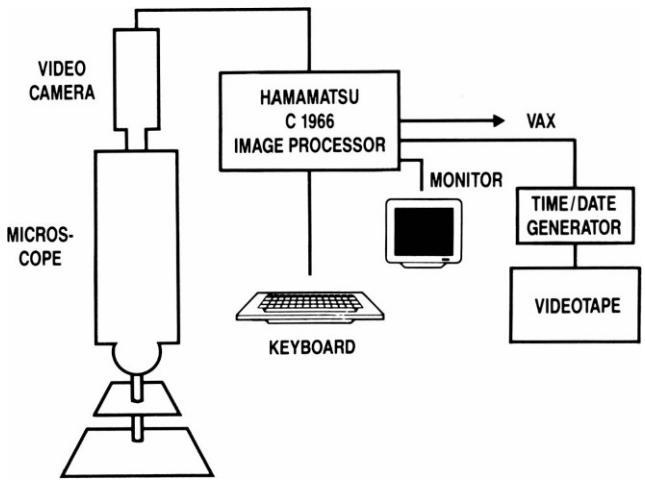

FIGURE 1 Block diagram of the set-up. The images in the Polyvar microscope are picked up by a Hamamatsu video camera and are digitized in the Hamamatsu C1966 Image Processor. The enhanced images are then transferred to a Sony VO-5850 P videotape and read back by the Image Processor into the VAX computer.

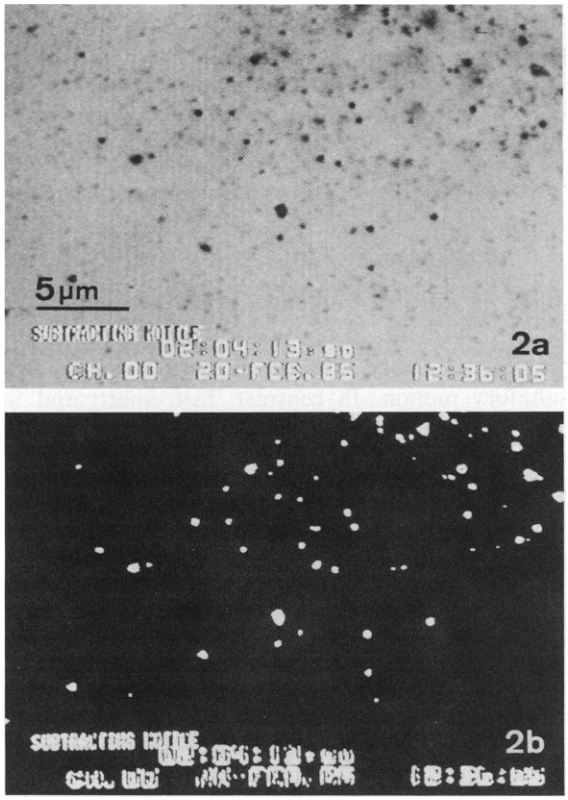

FIGURE 2 Example of bit-slicing the video image. Image *a* is a complete 256 gray-level bright-field image of the PTK_2 cellular system. In image *b*, the bit-slice window clearly extracts only the positional information of the colloidal gold particles. Figs. 2 and 3 are taken directly from the video screen. Scale bar, 5 μm.

$$M_2(n_0,n_1) = \sum_{i=1}^{512}\sum_{j=1}^{512}[(i-256)^2 + (j-256)^2]\, w_{ij}$$

Here $w_{ij} = 1$ if the pixel value is $n_0 \leq f_{ij} \leq n_1$ and $w_{ij} = 0$ if this condition is not met. In this way we can keep very easily all positional information on the colloidal gold particles while achieving a high data compression. The time indications at the bottom of the image are read by using a template-matching algorithm (Tov and Gonzales, 1974), but can be corrected if necessary. The stored series of images are sorted accordingly and this information is kept in a separate file. We mostly end up with a sequence of some 100 image files covering a time interval of 40–60 s. This information can be compressed in ~2 MByte of disk memory.

Tracking the Particles

The second part of the technique is a fully automatic tracking program. According to the sorting file, the image frames are read in the correct time sequence and decompressed. In the first frame, all pixel values clustered to the image of the same colloidal gold particle are classified and enumerated according to the mass-center of the cluster. In each subsequent frame, we use the position of the particle in a previous frame for detecting new clusters in a small square area. The size of the area is increased until no clusters touch the boundaries anymore. From the collection of found particles including those of the RESCUE matrix (see below), the hit nearest to the old position is retained as the new position, if the distance covered in this time interval is less than a certain value. We can get a reasonable upper limit for this value, by keeping in mind that the maximal velocity for saltatory jumps is ~3–4 μm/s, which gives ~9–12 pixel in our interframe time interval.

If the nearest hit does not satisfy this condition, it is placed together with the others in a RESCUE matrix. The grey-level values of these pixels are adapted so that they are counted only once. After all hits have been localized, the program looks at which hits could be related to some particles two frames earlier and which apparently have disappeared in the intermediate frame. This could be due to a fluctuation in intensity which slides the particle just outside the histogram window. Careful examination of the video frames shows that this phenomenon often appears with "grey" particles, which probably are just on the boundary of the focus plane.

After all previous hits have been exhausted, the remaining hits are placed in new slots of the coordinate matrix. They are supposed to be the beginning of new tracks of colloidal gold particles. They can be regarded as particles coming in focus and getting enough contrast to be counted in the mask on the gray-level histogram.

By choosing the nearest distance as the central key decision, we are aware that we are biasing the mobility towards smaller values, but it keeps the crossing error probability (the probability that we confound the track of two particles) at a very low level.

We end up with the coordinates of the particles at subsequent times, an information of a mere 150 kByte. The total time for this tracking algorithm is <1 s per particle coordinate, so that we can track 60 particles over 100 frames in ~ 1 h cpu time. This is routinely performed overnight in a batch mode.

Statistical Analysis of the Mobility

Statistical analysis is performed by taking into account the typical pattern of saltatory and Brownian motion. Saltatory movement is characterized by long (>1 μm) linear jumps, interleaved by rather long stop times (2–5 s), whereas Brownian motion is more a rocking motion with small elongations and no stop times. This qualitatively delineates the criteria for both types of motion (Freed and Verowitz, 1972).

By assuming a uniform kinetic motion, the jump velocity was calculated as the ratio of jump length to jump time.

The linearity of the saltatory motion is analyzed by checking that the new direction lies within 30° of the former directions. If this is not the case, the previous jump is considered finished and is classified as saltatory if the jump time exceeds 1.5 s or the distance is more than 1 μm. In this way distributions of jump time, jump velocity, jump directions, and stop times are continuously updated as we run through the coordinate matrix.

If the motion was not saltatory, we classified it as random motion. At the end of the frames, we collected all random motions of the same

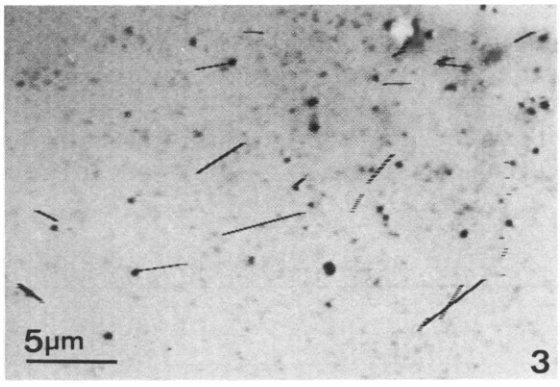

FIGURE 3 Tracks generated by the technique on a full morphological image of a PTK-2 cell, injected with 40-nm colloidal gold. The tracks display the real jumps of the particles in their saltatory motion as analyzed in a 50-s tape duration. That some tracks do not seem related to any particle displayed is because the particle could have performed some random motion just before the saltation or have just come into focus at that moment.

particle and performed a linear regression on the $\langle x^2 \rangle$ spreading factor versus elapsed time. Only those motions that provided a regression coefficient of more than 0.8 on more than 5 points were accepted. Therefore the probability of including a drift component was minimized. The slope of this linear regression is proportional to the diffusion coefficient.

Finally, we have the possibility to display the recovered tracks on the Hamamatsu video screen to assess visually the tracking activity (Fig. 3). We can then eventually examine the real videotape to assess the status of these tracks.

Brownian Motion by Spreading after Microinjection

The study of Brownian motion by spreading after microinjection is completely different from the former approach and is merely a concentration technique, which makes it similar to the classical fluorescence approaches (Brink and Ramanan, 1985). We used it to test our measurement of Brownian mobility based on the movement of individual particles. After microinjection in the cell at V_0 (i_0, j_0), the spreading of the colloidal gold was assessed by considering the diffusion equation in a two-dimensional plane. For this type of measurement, we must find a value that is proportional to the concentration of molecules. Because the colloidal gold is very well contrasted as black dots against a white background, the pixel values of the negative bit-sliced image are taken as the appropriate concentration. We then calculate the value

$$\langle r^2 \rangle = \sum_{i=1}^{512} \sum_{j=1}^{512} f_{ij} [(i - i_0)^2 + (j - j_0)]^2 / f_0,$$

where f_{ij} is the pixel value at (i, j), (i_0, j_0) is the point of microinjection, and

$$f_0 = \sum_{i=1}^{512} \sum_{j=1}^{512} f_{ij}.$$

If we assume a two-dimensional diffusion we find that

$$\langle r^2 \rangle = r_0^2 + 4\,Dt \qquad (1)$$

from which we can calculate a value for D (Crank, 1975).

RESULTS

Simulated Data

The whole concept has been extensively tested on simulated data. We therefore constructed a sequence of images with moving particles, ranging in size from 1 to 36 pixel. The particles performed only saltatory motion with well-defined jump and stop times each on its own direction, chosen within 10 random orientations. A number of bit-sliced images is put on disk and is analyzed by the second and third part of the program. We observed that from 50 particles on, the probability of crossing tacks raises to ~5%. For this reason, we tried to keep the number of the actual observed particles <30.

Real Data

With the in vitro microtubule system, we observed two types of movement. Long smooth unidirectional tracks with uniform velocity, interleaved by stops were classified as saltatory motion. In contrast, fast, short, and jerky motions in the two directions along the linear microtubules were regarded as random motions. We observed a marked dependence of the presence of ATP on the relative number of moving particles (saltatory as well as random). Indeed, in the preparations without added ATP, the relative number of moving particles dropped markedly (see also Table I). In the presence of AMP-PNP, a nonhydrolyzable ATP analogue, we even observed no motion at all. In the cellular system, saltatory motion was observed as long (sometimes over several seconds) tracks along linear paths; in contrast, the rocky shorter movements, which showed no net displacement, were classified as random motions.

Saltatory Motion. The distributions of jump times and jump velocities of the saltatory motion in the in vitro microtubule system were compared with those obtained by tedious manual tracking. Table I lists some features of these saltatory motions obtained both with manual and automatic tracking. It is clear that the automatic approach gives fairly good results.

Figs. 4 and 5 show the jump times and stop times distributions on this same system. The large form of the distribution can partly explain the rather large variance of the mean velocity.

In the PTK-2 cells, we observed some saltatory movements of colloidal gold markers. These arise probably by association of gold particles with vesicles and subsequent attachment on the microtubule system. It is evident from the values in Table I that the mean velocity in the cellular system lies in the order of 1 μm/s. This result agrees

TABLE I
STATISTICAL ANALYSIS OF SALTATORY MOTION IN THE TWO DIFFERENT EXPERIMENTAL SITUATIONS

	Total No. of particles observed	Mean velocity	Fraction of moving particles	Duty cycle
		$\mu m/s$	%	
Microtubules, with ATP manual	109	0.51 ± 0.2 (21)	54	—
Microtubules, with ATP automatic	113	0.55 ± 0.3 (31)	57	0.172
Microtubules, without ATP manual	121	—	21	—
Microtubules, without ATP automatic	315	—	14	—
AU-40 in PTK-2 cells	85	1.12 ± 0.4 (15)	45	0.221

In parentheses are the number of particles studied for that specific movement. The fraction of moving particles refers to both saltatory and Brownian motion.

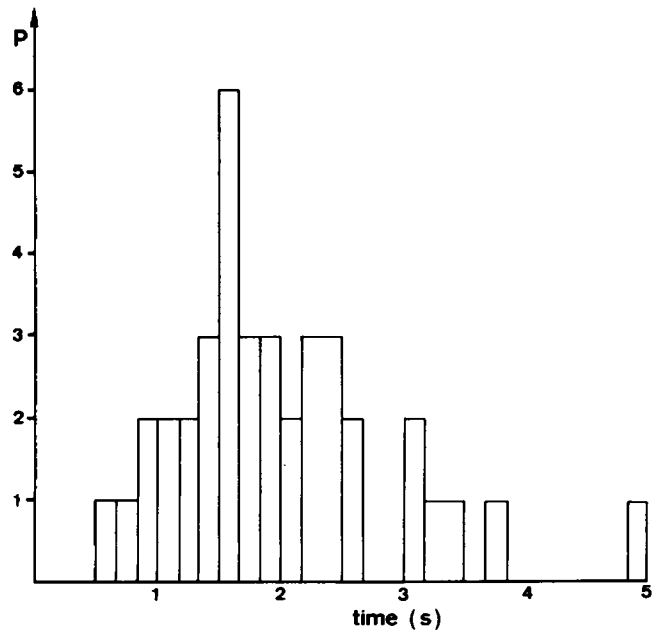

FIGURE 4 Jump time distribution of 39 saltatory movements in the in vitro microtubuli system.

quantitatively with the manual analysis of moving organelles and injected gold (De Brabander et al., 1986).

An interesting parameter in the study of the energy requirement of the saltatory movement is the so-called "duty-cycle." We define it as the sum of the jump times of all observed movements divided by the total time all moving particles were observed. This gives an indication of the relative amount a particle is participating in the energy-demanding saltatory movement at any moment.

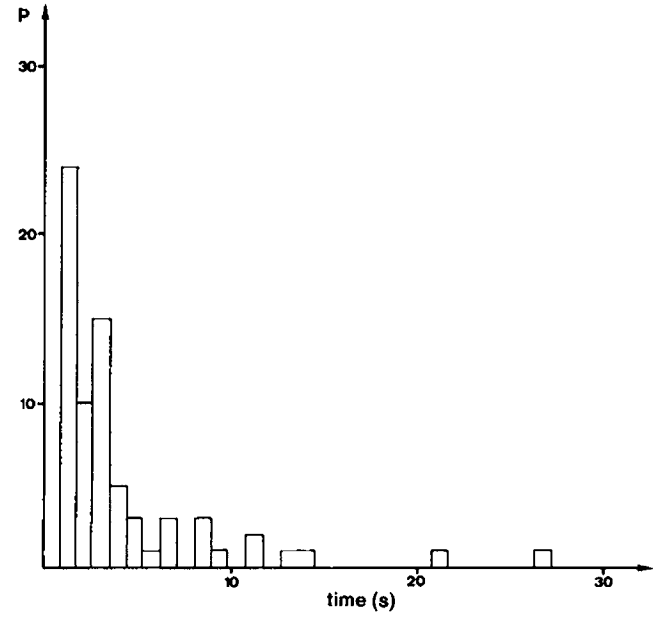

FIGURE 5 Stop time distribution of the same in vitro microtubule system. The tape was examined for a total duration of 55 s.

TABLE II
ANALYSIS OF THE BROWNIAN MOTION IN THE MODEL SYSTEM AND AFTER INJECTION IN PTK CELLS

	Diffusion coefficient	No. of particles observed
Microtubule system with ATP	$\mu m/s$	
Automatic	0.42 (1)	30
Manual	—	22
Microtubule system without ATP		
Automatic	0.32 (1)	39
Manual	—	20
PTK-2 cells, tracking	0.28 (2)	20
PTK-2 cells, spreading	0.15 (2)	—

Results refer to the value of the diffusion coefficient and are given in $\mu m^2/s$. The numbers in parentheses refer to the dimension of the movement (linear, plane, . . .).

Random Motion. From those movements, which were not classified as saltatory motion, we state that the values of the slope of the regression line in the $\langle x^2 \rangle$ versus t plane are equal to $2nD$, where n is the dimensionality of the movement and D the diffusion coefficient.

It is clear from visual observations in the in vitro system that the observed random movement is mainly one-dimensional, a result we will illustrate below. Table II lists the diffusion coefficients in the cases with and without ATP. We can then assign a dimensionality of the movement to this particle in the following manner.

The program lists the distribution of orientations and their variances of this random movement for each gold particle (Table III). Because the absolute value of most variances is very low (<30°), we can assign a linear character to these motions.

In contrast, in the cellular system a significantly larger

TABLE III
MEAN ORIENTATIONS (MODULO 180°) AND VARIANCES OF THE CONSECUTIVE MOTIONS OF ONE PARTICLE AS OBSERVED IN THE TWO EXPERIMENTAL SYSTEMS AND CLASSIFIED AS RANDOM MOTIONS

Microtubules in vitro (30 movements observed)	AU-40 in PTK_2 cells (20 movements observed)
56.7 ± 7.5 (6)	120.9 ± 28.2 (5)
98.5 ± 7.5 (9)	122 ± 31.2 (7)
49.6 ± 16.6 (7)	102 ± 32.9 (6)
76.6 ± 16.8 (5)	45.0 ± 33.8 (5)
78.8 ± 19.2 (6)	112 ± 40.1 (6)
54.4 ± 20.2 (7)	90.1 ± 42.8 (7)
73.8 ± 22.9 (5)	92.6 ± 48.2 (5)
42.4 ± 23.2 (8)	120.4 ± 54.4 (7)
103.6 ± 27.2 (7)	88 ± 71 (6)
122.8 ± 31.8 (8)	112 ± 71 (6)

Only the first 10 motions with increasing variance in orientation are presented. All data are in degrees. In parentheses are the number of jerky movements the program has recorded of that specific particle. It is clear the many more movements in vitro exhibit a small variance of orientation, suggesting mainly one-dimensional motion.

population (60–70%) showed a larger relative variance of the orientations, which suggests a more two-dimensional diffusion behavior also assumed by photobleaching experiments (Woscieszin et al., 1987).

In this context it must be stated that the algorithm automatically detects when a particle goes out of focus. This is mainly achieved in two ways: either the pixel value diminishes sufficiently to make the signal drift out of the bit-slice window, or the size of the particle increases dramatically when the particle goes out of focus (the so-called blurring effect). In both cases, the motion of the particle is not taken into account, because a clear stop point is not determined. Furthermore, the thickness of the PTK_2 cell (1 μm on the peripheral lamella to 4–5 μm thickness above the nucleus) keeps most particles in focus, given the depth of focus at this magnification (1–2 μm). This guarantees that, at least for the particles retained by the program, the assumption of two-dimensional behavior can hold. Fig. 6 shows the $\langle r^2 \rangle$ versus t plot in the spreading approach of microinjected colloidal gold. A fit of these values, according to Eq. 1 yields a diffusion coefficient D_C of 0.15 $\mu m^2/s$. A problem with this technique, however, is that the particles begin to spread only after a certain time of observation. They remain clustered for a certain number of minutes, so a clear time origin cannot be given. Fig. 7 then shows this diffusion coefficient along with the distribution of random mobilities as assessed from the tracking algorithm at 2.30 h after microinjection. This mean value falls well within the distribution. A spherical particle of that diameter in water has a diffusion coefficient D_W of ~10 $\mu m^2/s$. We see that the retardation factor D_W/D_C is ~100, which is qualitatively in agreement with photobleaching experiments (Gershon et al., 1985; Jacobson and Wosciezyn, 1984).

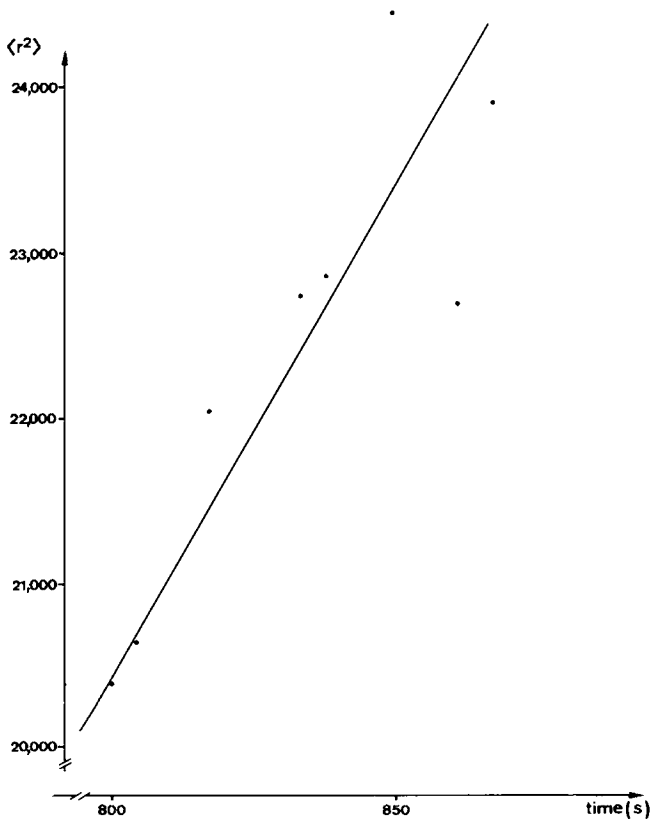

FIGURE 6 $\langle r^2 \rangle$ versus t in the microinjection technique. $\langle r^2 \rangle$ is given in pixel², where at the given magnification 1 μm equals 9.4 pixel. The slope therefore is equal to 53 pixel²/s, and from Eq. 1, the diffusion coefficient D = 13.25 pixel²/s or 0.15 $\mu m^2/s$. Careful observation of the images show that the particles stay clustered a certain number of minutes after injection, so that the effective spreading begins much later than suggested by the $t = 0$ origin of the figure.

DISCUSSION

The proposed method allows one to study the features of the mobility of individual marker particles, in contrast with classical photobleaching techniques which yield information on the behavior of a large group of molecules.

The tracking approach gives complete statistics of saltatory motion in living cells including the distribution of stop times. This information is absolutely necessary in the search for the molecular mechanism of saltatory motion (Weiss and Gross, 1982, 1983; Vale et al, 1985; Allen et al., 1985). Indeed, much evidence suggests that the movements of colloidal gold probes along microtubules are guided by the same mechanism as the movement of endogenous organelles. First, the negatively charged colloidal gold probes, when microinjected into cells, associate with the microtubular system and begin to saltate. Second, the mean velocity of this movement is closely related to the velocity of moving endogenous organelles, such as vesicles (De Brabander et al., 1985). Furthermore, we have shown

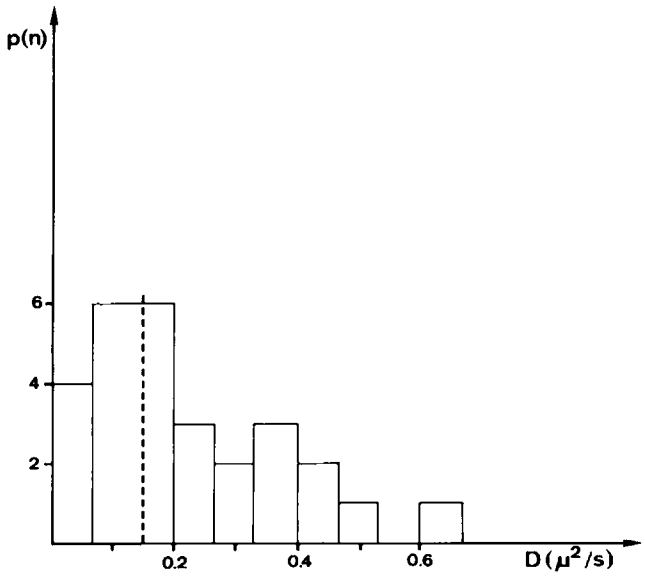

FIGURE 7 Distribution of the diffusion coefficients of 40-nm gold microinjected into PTK-2 cells and assumed to diffuse in the cytoplasm. The mean value, determined by the spreading technique, is shown as a full line.

in this report that the automatic tracking program yields reasonable values for the velocity and jump times of saltatory motion (Freed and Verowitz, 1972).

An interesting parameter is the so-called duty cycle figure, which gives the amount of time each individual marker molecule is in saltatory motion. For the systems under study, we see that there is a clear dependence of this figure on the presence of ATP.

A very exciting feature of this tracking approach is the simultaneous measurement of random motion, based on the tracks of individual markers. The orientation of the tracks gives a good idea about the dimensionality of the random movement. In this way, we can distinguish between linear random motion along microtubules and two-dimensional random motion in the cytoplasm.

For the case of the microtubular system in vitro, we see that the linear diffusion coefficient along the microtubules drops to ~5% of its value in the same isotropic solution. This points towards a certain retention of the gold probe on the microtubular structure, the molecular mechanism of which we are currently investigating.

For the random diffusion in the PTK-2 cellular system, we compared the tracking approach to the more classical spreading after microinjection. We could indeed observe random motion of single particles in the same experimental system. The apparent discrepancy between the two results (Fig. 7) can be associated partly to the large distribution as measured by the tracking approach, which is probably due to aggregation and association with vesicles.

Another point is the assumption of the two-dimensional data analysis itself. Careful examination of the mean orientation and relative variance of the "random tracks" indicate that ~25% of the particles are moving in a "linear fashion" (see the first four entries in Table III), probably along the microtubular system (similar to the in vitro system). Although the coating of the gold probes with cetydylpyridine in principle prevents them from association with the positively charged microtubules, we cannot exclude that some gold particles have been insufficiently coated. Also, some positively charged gold particles associated with endogenous vesicles and displayed saltatory behavior in a piggy-back fashion. These observations can have far reaching consequences, because they will interfere with the assumption of planar and free two-dimensional diffusion in photobleaching experiments.

A last comment can be made. Because we observe the individual random motion of particles, we can investigate the presence of barriers to this diffusion and the aspecific interactions (if they are strong enough to stop the motion).

Concerning the tracking strategy, one could wonder why we don't use the more "classical" tracking approach by essentially taking the difference of subsequent frames and getting a high contrast between moving parts and the stationary background. The reason is twofold. First the NANOVID technology in itself procures a satisfactory contrast. Second, the latter approach is not capable of getting information on stop times of immobile particles, an important feature in the study of any motion.

We may compare the features of the NANOVID approach with those of the classical fluorescence microscopic techniques. In some cases individual fluorescent complexes may be visualized and their mobility studied. This is the case for mitochondria stained with rhodamine 123 (Salmeen et al., 1985), and for fluorescently labeled low density lipoprotein (LDL) complexes (Webb and Gross, 1987). In all these cases, the moving complexes were quite large (40–1,000 nm), or quite exceptional (i.e, LDL-receptor). In contrast, the colloidal gold together with the coupling to antibodies permits the visualization of the variety of complexes down to 20 nm, as is the case for a monoclonal antibody against the transferrin receptor (De Brabander et al., 1986), or for the study of membrane probes (Geerts et al., 1987).

Another point concerns the specificity of labeling, which is in general much better for fluorescent probes. Indeed, studies of the binding of fluorescently tagged Fab antibody do not suffer from the problems with multivalent binding–induced cross-links. Because the number of Fab antibody fragments coupled to one colloidal gold particle is not known in advance, multivalent cross-linking can be induced, thereby interfering with the determination of exact binding kinetics.

The greater power of fluorescent techniques is without discussion its spectral sensitivity to microenvironmental parameters, such as pH, calcium concentration, and membrane potential, an exciting area, which is growing quite fast. Furthermore, measurements of fluorescence depolarization are able to probe microfluidity and the extension of this technique to phosphorescence will prove to be of major importance in the studies of membrane protein aggregation.

In contrast, the great contribution of the NANOVID approach is the realization that the spectrum of movement of one molecule is at the same time very complex (Brownian motion in one or two dimensions, saltations, periods of stops) and very heterogeneous, in various parts of the cellular system.

An important point can be made concerning the specific density of colloidal gold. In fact, the Brownian diffusion coefficient is independent of the mass of the particle, and related to the radius (Einstein, 1908; Saffman, 1976). This means that colloidal gold particles are excellent probes of random motion, because their mass does not interfere with the translational dynamics.

Furthermore, NANOVID allows one to study the movement against a visible morphological localization of the particles with regard to different subcellular structures. Also, the technique is not hampered by cellular autofluorescence which in some cases can be very important. The NANOVID tracking method allows one to investigate clearly the dimensionality of movements, a very important

parameter, especially for the study of the effect of reduction of dimensionality in the rates of diffusion-controlled reactions, a controversial topic (Adam and Delbruck, 1968; Hardt, 1979; McCloskey and Poo, 1986).

In summary, we can clearly state that the NANOVID-tracking approach provides a wealth of information on the different types of motion, which is fully complementary with the classical spectroscopic techniques. We feel that this is only a grasp of the power of these techniques and we believe that the development of even more powerful and lower cost hardware will extend the availability of this technique.

The skillful photography of L. Leijssen and his group is highly appreciated. Further thanks go to C. Geentjens for secretarial assistance.

This work was supported by I. W. O. N. L. (Brussels, Belgium).

Received for publication 9 June 1986 and in final form 4 May 1987.

REFERENCES

Adam, G., and M. Delbruck. 1968. Reduction of dimensionality in biological diffusion processes. *In* Structural Chemistry and Molecular Biology. A. Rich and N. Davidson, editors. Freeman W.H. New York.

Allen, R., J. Travis, N. Allen, and H. Yllmaz. 1981. Video-enhanced contrast polarization (AVEC-POL) microscopy: a new method applied to the detection of birefringence in the mobile reticulopodial network of Allogramic laticollaris. *Cell Motil.* 1:275–289.

Allen, R., D. Weiss, J. Hayden, D. Brown, H. Fujiwake, and M. Simpson. 1985. Gliding movement of the bidirectional organelle transport along single native microtubules from squid axon axoplasm: evidence for an active role of microtubules in cytoplasmic transport. *J. Cell Biol.* 100:1736–1753.

Ansorge, W. 1982. Improved system for capillary micro-injection into living cells. *Exp. Cell Res.* 140:31–37.

Axelrod, D., D. Koppel, J. Schlessinger, E. Elson, and W. Webb. 1976. Mobility measurements by analysis of fluorescence recovery after photobleaching. *Biophys. J.* 16:1055–1069.

Barak, L., and W. Webb. 1982. Diffusion of low-density lipoprotein-receptor complex on human fibroblasts. *J. Cell Biol.* 95:846–852.

Brink, P., and S. Ramanan. 1985. A model for the diffusion of fluorescent probes in the septate giant axon of the earthworm. Axoplasmic diffusion and functional membrane permeability. *Biophys. J.* 48:299–309.

Crank, J. 1975. The Mathematics of Diffusion. Clarendon Press, Oxford. 414 pp.

De Brabander, M., R. Nuydens, G. Geuens, M. Moeremans, and J. De Mey. 1985. Probing microtubule-dependent intracellular motility with nanometer particle video ultramicroscopy (Nanovid ultramicroscopy). *Cytobios.* 43:273–283.

De Brabander, M., R. Nuydens, G. Geuens, M. Moeremans, and J. De Mey. 1986. The use of submicroscopic gold particles combined with video contrast enhancement as a simple molecular probe for the living cells. *Cell Motil. Cytoskeleton.* 6:105–113.

De Brabander, M., R. Nuydens, H. Geerts, J. De Mey, M. Moeremans, and C. Hopkins. 1986. Intracellular routing of receptosomes observed in living cells using Nanovid microscopy. *J. Cell Biol.* 103(5, Pt.2):61a. (Abstr.)

De Mey, J. 1983. Colloidal gold probes in immunocytochemistry. *In* Immunocytochemistry. Polak, editor. Van Noorden, London-Wright PSG. 92–110.

Einstein, A. 1908. Elementare theorie der Brownsche Bewegung. *Z. Electrochem.* 14:235–239.

Elson, E., and D. Magde. 1974. Fluorescence correlation spectroscopy. I. Conceptual basis and theory. *Biopolymers.* 13:1–27.

Freed, J., and M. Verowitz. 1972. The association of a class of saltatory movements with microtubules in cultured cells. *J. Cell Biol.* 45:334–354.

Geerts, H., M. De Brabander, R. Nuydens, J. De Mey, and R. Nuyens. 1987. Nanovid correlation spectroscopy: quantitative analysis of cell surface motility with poly-lysine coated gold particles. Abstract for the 9th International Biophysics Congress, Jerusalem.

Gershon, N., K. Porter, and B. Trus. 1985. The cytoplasmic matrix: its volume and surface area and the diffusion of molecules through it. *Proc. Natl. Acad. Sci. USA.* 82:5030–5035.

Hardt, S. 1979. Rates of diffusion controlled reactions in one, two and three dimensions. *Biophys. Chem.* 10:239–243.

Inoué, S. 1981. Video-image processing greatly enhances contrast, quality and speed in polarization-based microscopy. *J. Cell Biol.* 89:346–356.

Jacobson, K., and J. Wosciezyn. 1984. The translational mobility of substances within the cytoplasmic matrix. *Proc. Natl. Acad. Sci. USA.* 81:6747–6751.

Kapitza, H., G. McGregor, and K. Jacobson. 1985. Direct measurement of lateral transport in membranes by using time-resolved spatial photometry. *Proc. Natl. Acad. Sci. USA.* 82:4122–4126.

Magde, D., and E. Elson. 1974. Fluorescence correlation spectroscopy. II. An experimental realization. *Biopolymers.* 13:29–61.

McCloskey, M. and M. Poo. 1986. Rates of membrane-associated reactions: reduction of dimensionality revisited. *J. Cell Biol.* 102:88–97.

Murphy, D., and G. Borisy. 1975. Association of high molecular weight proteins with microtubules and their role in microtubule assembly *in vitro. Proc. Natl. Acad. Sci. USA.* 72:2696–2700.

Peters, R. 1984. Nucleo-cytoplasmic flux and intracellular mobility in single hepatocytes measured by fluorescence microphotolysis. *EMBO (Eur. Mol. Biol. Organ.) J.* 3:1831–1836.

Saffman, P. 1976. Brownian motion in thin sheets of viscous fluid. *J. Fluid Mech.* 73:593–602.

Salmeen, I., P. Zacmanidis, G. Jesion, L. A. Feldkamp. 1985. Motion of mitochondria in cultured cells quantified by analysis of digitized images. *Biophys. J.* 48:681–686.

Smith, B., W. Clark, and H. McConnell. 1979. Anisotropic molecular motion on cell surfaces. *Proc. Natl. Acad. Sci. USA.* 76:5641–5644.

Tov, P., and F. Gonzales. 1974. Pattern Recognition Principles. Chapter 4. Addison-Wesley Publishing Co. Inc., Reading, MA.

Vale, R., T. Reese, and M. Sheetz. 1985. Identification of a novel force-generating protein, kinesin, involved in microtubule-based mobility. *Cell.* 42:39–50.

Webb, W., and D. Gross. 1987. Patterns of individual molecular motions deduced from fluorescent image analysis. *In* Applications of Fluorescence in Biomedical Sciences. D. Taylor, A. Waggoner, R. Murphy, F. Camri, and R. Birge, editors. Alan R. Liss Inc., New York. 405–442.

Weiss, D., and G. Gross. 1982. The microstream hypothesis of axoplasmic transport characteristics. Predictions and compatibility with data. *In* Axoplasmic Transport. D. Weiss, editor. 363–375.

Weiss, D., and G. Gross. 1983. Intracellular transport in axonal microtubular domains. I. Theoretical considerations on the essential properties of a force-generating mechanism. *Protoplasm.* 114:179–197.

Wosciezyn, J., R. Schlegel, E. S. Wu, and K. Jacobson. 1981. Diffusion of injected macromolecules within the cytoplasm of living cells. *Proc. Natl. Acad. Sci. USA.* 78:4407–4410.